Date	Time	Room	Lecture Note
2010			
Sep. 21	14:00	B1A	Lecture 1-2
Oct. 5	14:00	244	Chapt-1
Oct. 8	14:00	244	Chapt-2
Oct. 12	14:00	N725	Chapt-3
Oct. 15	14:00	244	CANCEL!!
Oct. 22	14:00	244	Chapt-4
Oct. 26	14:00	244	Chapt-5,6
Oct. 29	14:00	244	CANCEL!!
Nov. 2	14:00	244	Chapt-6,7
Nov. 9	14:00	N725	Chap 7-8
Nov. 12	14:00	244	
Nov. 16	14:00	244	
Nov. 19	14:00	244	
Nov. 30	14:00	244	
Dec. 7	14:00	244	
Jan 4	14:00		
Jan 11, 2011	Final exam		

Spring semester (Beginning Feb 21, 2011)
Feb 22

Chapter 7 SCALAR COUPLING

Scalar couplings arise from spin-spin interactions that occur via bonding electrons. Consequently, they provide information on the chemical connectivity between atoms. Therefore, these couplings can be utilized to correlate NMR signals of atoms that are chemically bonded to one another, providing chemical shift assignments if the molecular structure is known. In particular, the scalar coupling across the peptide bond permits the linkage of spins within one amino acid to those of its neighbors.

In addition to providing information on chemical connectivities, the sizes of three bond scalar couplings are sensitive to the electron distribution of the intervening bonds, consequently these couplings can provide information on the conformation of rotatable bonds in proteins.

Scalar, or J-coupling, occurs between nuclei which are connected by chemical bonds. This coupling causes splitting of the spectral lines for both coupled spins by an amount J, or the coupling constant. The nomenclature that is used to describe the coupling is as follows: ${}^{n}J_{AB}$

where n refers to the number of intervening bonds, and A and B identify the two coupled spins. For example, the coupling constant between the amide nitrogen and the Cβ carbon would be written as: ${}^{2}J_{NC\beta}$. The value of J is usually given in Hz and is the observed frequency separation between the split resonance lines of the coupled spins.

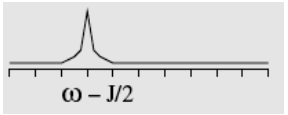

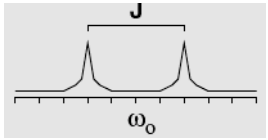

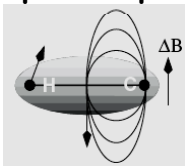

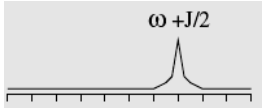

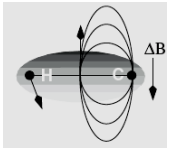

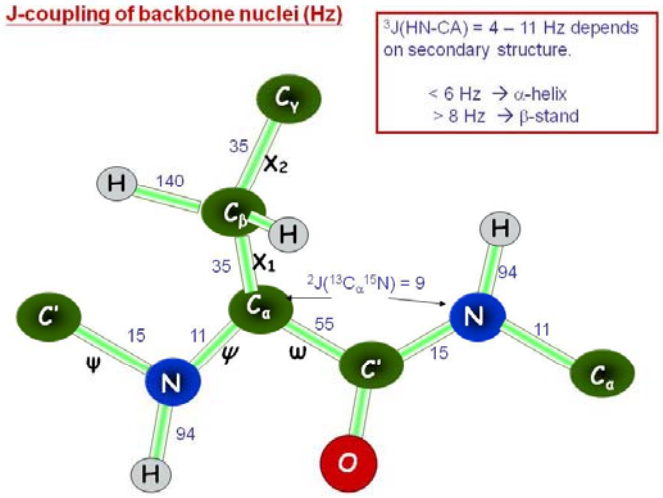

The effect of J-coupling on the spectrum depends on the frequency separation of the coupled spins. If the two coupled spins differ greatly in their resonance frequencies ($\Delta\nu > J$), then the system is referred to as an AX system, where the X signifies the fact that the two chemical shifts are quite different. All coupling between different atom types, or heteronuclear spins, are AX couplings because of the large difference in the frequencies of coupled spins. Examples include, J_{NH}, J_{CH}, and J_{NC}. AX couplings can be analyzed using a classical analysis, similar to that depicted in Fig. 7.1. When two coupling spins have nearly equivalent resonance frequencies ($\Delta\nu \leq J$) then the system is referred to as an AB system. For example, the coupling between two H_β protons on an amino acid is an example of an AB system. Accurate analysis of AB systems require a detailed quantum mechanical treatment. Lastly, when the coupled spins have the identical resonance frequencies, the observed coupling disappears entirely. This is most often seen when multiple protons have equivalent environments, such as the three protons on a methyl group.

7.2 Basis of Scalar Coupling: Scalar coupling arises from the interaction of the nuclear magnetic moment with the electrons involved in the chemical bond. The nuclear spin polarization of one atom affects the polarization of the surrounding electrons. The electron polarization subsequently produces a change in the magnetic field that is sensed by the coupled spin..

Table 7.1. Homonuclear and heteronuclear coupling constants. The values are approximate; the coupling constants will also be affected by the electronic environment of the associated spins.

Couplings Involving Heteronuclear (^{13}C or ^{15}N) Spins		*Proton-Proton Couplings*	
C-N	14 Hz	H-C-H	-12 to -15 Hz
C-C	35 Hz	H-C-C-H	2-14 Hz
H-N	92 Hz	H-C=C-H	10 (cis)/17 (trans)
H-C	130 Hz	H-N-C-H	1-10 Hz
H-C-C	5 Hz (two bond coupling)		(3 Hz α-helix)
			(10 Hz β-strand)

$$\Delta\omega \propto \pm\gamma_H\gamma_C$$

The strength of the J-coupling depends on several factors, including the gyromagnetic ratio of the coupled spins, the number of bonds connecting the coupled spins, and the conformation of the intervening bonds in the case of multiple bond couplings.

In the case of multiple bond couplings, the conformation of the coupled atoms affects the coupling constant. For example, the three bond proton-proton coupling in the H-C-C-H group ranges from 2 to 14 Hz. The relationship between the coupling constant and the torsional angle is represented by the **Karplus relationship**:

$J = A\cos^2\theta + B\cos\theta + C$ where A, B and C are empirical constants.

For example, the φ angle in the peptide bond affects the strength of the coupling between the amide proton and the alpha proton, as illustrated in Fig. 7.2.

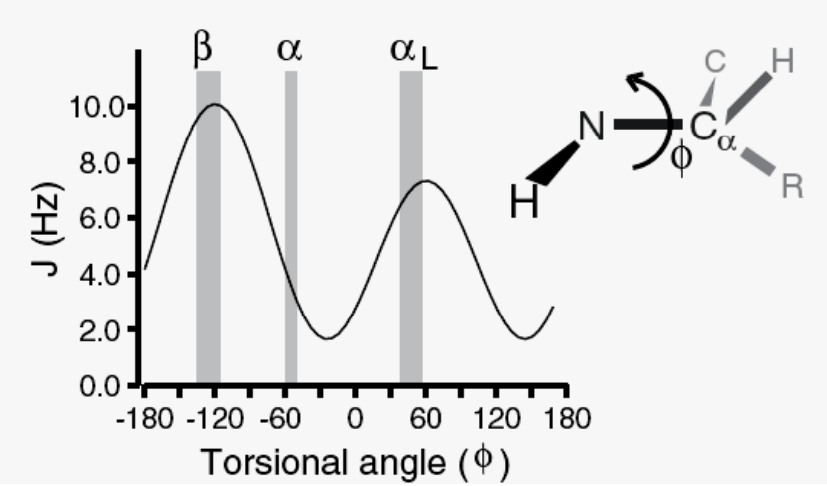

Figure 7.2 Karplus curve for a peptide group. The relationship between J and the φ torsional angle in polypeptides is shown. The φ angles for regular secondary structures are indicated by the vertical gray bars. The φ torsional angle is defined by the relative orientation of the H-N bond vector to the Cα-CO bond vector. The molecular fragment to the right of the plot has a φ angle of 180°.

$$J = 6.98\cos^2(\varphi-60) - 1.38\cos(\varphi-60) + 1.72$$

(Karplus equation)

7.2.1 Coupling to Multiple Spins

The coupling between a carbon and a hydrogen in a ^{13}C-H group results in the splitting of both the proton and carbon spectral line by an amount J_{CH} Hz. If the carbon atom is coupled to more than one equivalent proton1, such as in a $^{13}CH_2$ or $^{13}CH_3$ group, then a more complex splitting pattern is observed.

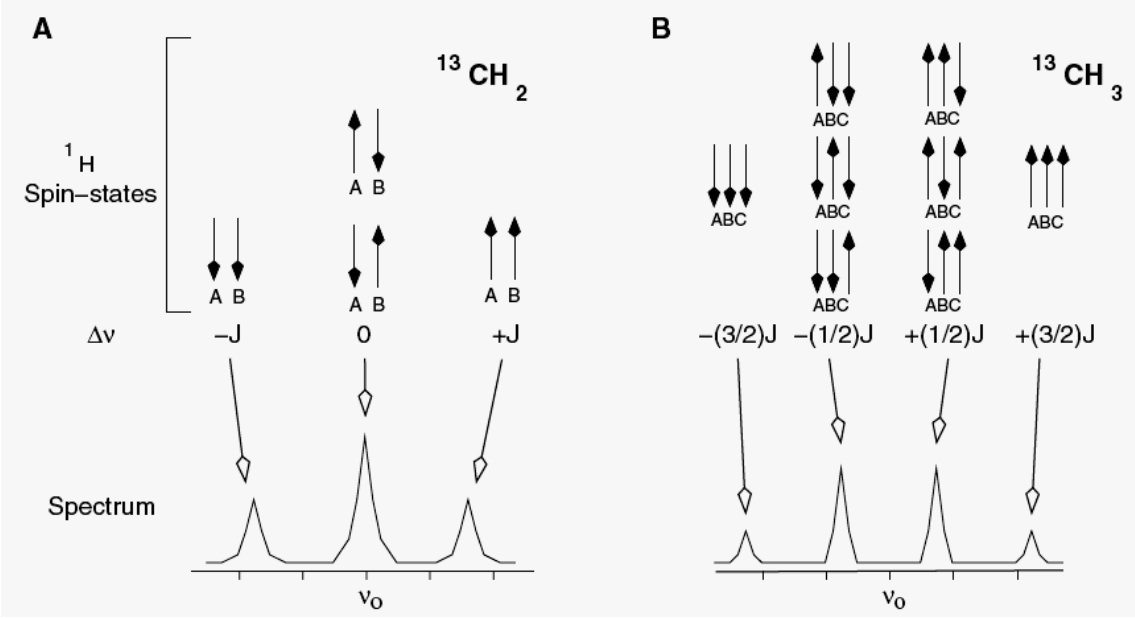

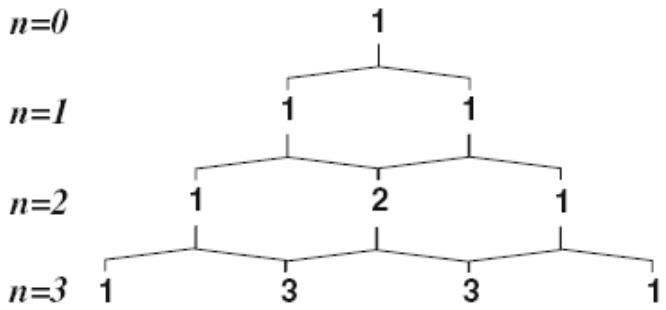

Figure 7.4 Analysis of J-coupling using Pascal's triangle.

Figure 7.3. Scalar coupling to multiple equivalent protons. The intensity of each line depends on the number of molecules in the sample with a particular spin state; a 1:2:1 ratio will be found for two coupled protons and a 1:3:3:1 ratio is found for three coupled protons.

In cases where an atom is coupled to two different, or non-equivalent, spins, then the couplings are treated independently. For example, the carbonyl carbon is coupled to both the amide nitrogen ($^1J_{NC'} \approx 12$ Hz) as well as the alpha carbon, ($^1J_{C'C\alpha} \approx 55$ Hz), consequently the spectral line from the carbonyl will be a quartet, showing both couplings.

Figure 7.5 Scalar coupling to nonequivalent spins. The spectrum of a carbonyl carbon is shown. A quartet is observed because the coupling to the alpha carbon ($J_{C\alpha}$) is larger than the two bond coupling to the nitrogen (J_{NC}). Since these four states are equally likely, the ratio of the intensities of the lines in the quartet are 1:1:1:1.

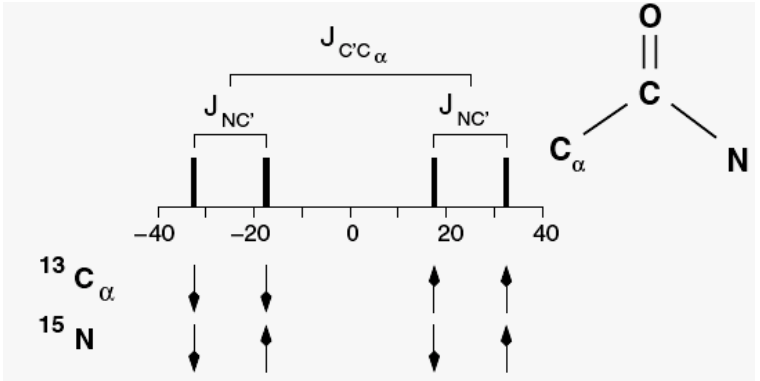

7.3 Quantum Mechanical Description

The Hamiltonian that describes scalar coupling between spins is given by: $\mathcal{H} = \vec{I}\ \tilde{J}\ \vec{S}$

The scalar coupling is represented by a tensor quantity which will be diagonal in some coordinate frame:

$$\tilde{J} = \begin{bmatrix} J_{xx} & 0 & 0 \\ 0 & J_{yy} & 0 \\ 0 & 0 & J_{zz} \end{bmatrix}$$

But isotropic rotation in solution ➔ $< J >= \frac{1}{3}[J_{xx} + J_{yy} + J_{zz}]$

So that J is a scalar quantity ➔ $\mathcal{H} = J\vec{I} \cdot \vec{S}$

7.3.1 Analysis of an AX System

The dot product, $\vec{I} \cdot \vec{S}$, expands to: $I \cdot S = I_x S_x + I_y S_y + I_z S_z$

In general, it would be necessary to use the complete expression for the dot product when analyzing the effect of the coupling on the energy states. However, if the frequency difference between the coupled spins is larger than the J-coupling, as is the case in an AX spin-system, then terms involving transverse operators can be dropped. This leads to a simplified representation of the Hamiltonian for a pair of coupled spins:

$H = -\omega_I I_z - \omega_S S_z + 2\pi J I_z S_z$ or in frequency units: $H = -\nu_I I_z - \nu_S S_z + J I_z S_z$

Before using this Hamiltonian to calculate the energy levels of the system it is necessary to write expressions for the basis states of the system. Four new states are generated by taking all possible combinations of the original basis vectors that were associated with each spin. These states are:

$$\phi_1 = |\alpha\alpha > \quad \phi_2 = |\beta\alpha > \quad \phi_3 = |\alpha\beta > \quad \phi_4 = |\beta\beta >$$

These wavefunctions are eigenfunctions of the uncoupled Hamiltonian. The first character (α or β) refers to the I spin while the second character refers to the S spin. In both cases α is associated with an m_z of +1/2, and β is associated with an m_z of -1/2

For example, $|\alpha\beta\rangle$ is a wavefunction in which the I spin has an m_z value of +1/2 and the S spin has an m_z value of -1/2. The four basis states form an ortho-normal basis set, e.g. $\langle \alpha\alpha|\alpha\alpha\rangle = 1$, $\langle\alpha\alpha|\alpha\beta\rangle = 0$.

The energy of each of these states is calculated directly from the Hamiltonian ($H|\Psi\rangle = E\Psi|\Psi\rangle$):

$$H|\varphi_1\rangle = (-\nu_I/2 - \nu_S/2 + J/4)|\alpha\alpha\rangle; \qquad H|\varphi_2\rangle = (+\nu_I/2 - \nu_S/2 - J/4)|\beta\alpha\rangle$$
$$H|\varphi_3\rangle = (-\nu_I/2 + \nu_S/2 - J/4)|\alpha\beta\rangle; \qquad H|\varphi_4\rangle = (+\nu_I/2 + \nu_S/2 + J/4)|\beta\beta\rangle$$

The four energy levels are illustrated in Fig. 7.6. Six different transitions are possible with this system. Of the six possible transitions, the following four are observable with equal intensity, (Single quantum transition) with the indicated energies:

$$E_{1\to2} = \nu_I - J/2; \qquad E_{1\to3} = \nu_S - J/2; \qquad E_{2\to4} = \nu_S + J/2; \qquad E_{3\to4} = \nu_I + J/2.$$

These transitions represent a normal 1D NMR spectrum between two coupled spins.

In addition to the above single quantum transitions there is also a double quantum transition: $E_{\alpha\alpha\to\beta\beta} = \omega_I + \omega_S$, and a zero quantum transition: $E_{\alpha\beta\to\beta\alpha} = \omega_I - \omega_S$, neither of which are directly observable since they involve an overall change in m_z of ±2 or zero.

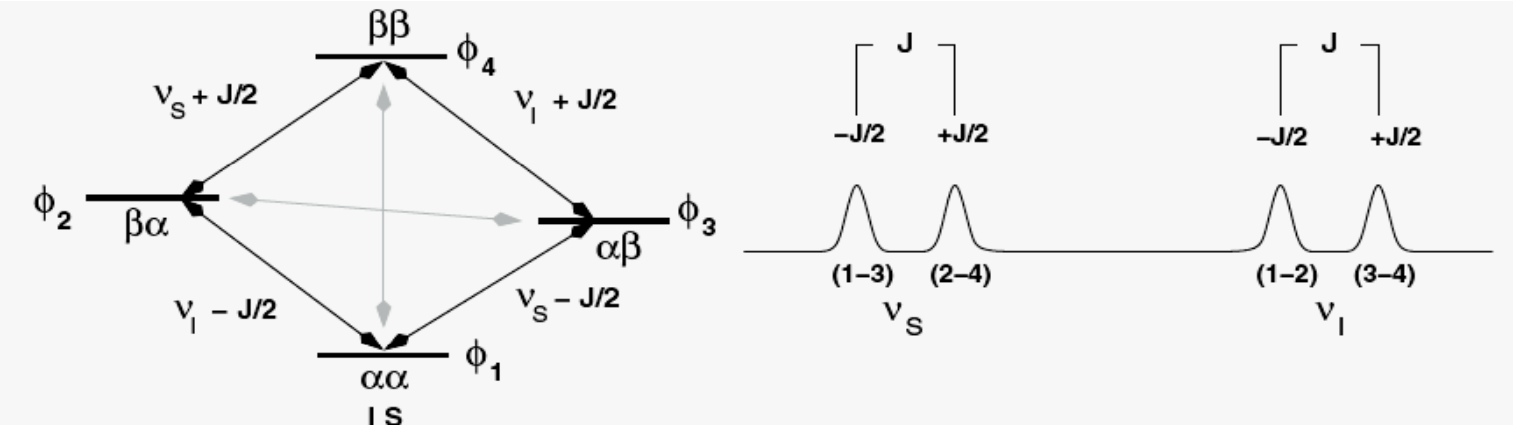

Figure 7.6. Energy levels and resultant spectrum for two coupled spins.

7.3.2 Analysis of an AB system

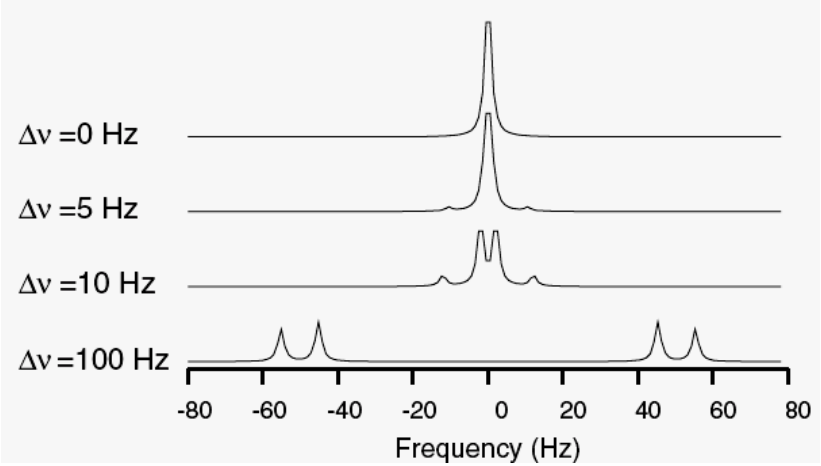

Figure 7.7 Effect of frequency separation on observed J-coupling. Simulated spectra are shown to illustrate the collapse of observed coupling as Δν becomes smaller than J. The J-coupling constant is 10 Hz, and the separation between the lines is decreased from 100 Hz (bottom spectrum) to 0 Hz (top spectrum).

7.4 Decoupling

Scalar coupling leads to splitting of spectra lines and therefore reduces the signal to-noise in the spectrum by spreading the intensity over all of the peaks in the multiplet. This loss in signal-to-noise can be restored by collapsing the multiplet to a single line by decoupling. Since the splitting arises from the influence of the magnetic state of one spin on the other, decoupling can be accomplished by simply inverting the spin-state of the coupled partner during detection. For example, in the case of a ^{13}CH group, if the carbon magnetization is inverted rapidly, the protons in the sample no longer sense two distinct carbon spin-states, but a single averaged state. One way of achieving this inversion is to simply apply a train of 180◦ pulses to the carbon, as illustrated in Fig. 7.8. More effective decoupling is obtained as the rate of inversion is increased by reducing both the inter-pulse spacing and the 180◦ pulse length.

7.4.1 Experimental Implementation of Decoupling

Figure 7.8. Averaging of spin states during decoupling. A series of π pulses can average spin states, removing the effects of spin-spin scalar coupling on the NMR spectrum (decoupling). The upper part of the figure shows the precession of a single proton in a CH or NH group. The lower segment shows a train of π pulses that are applied to the heteronuclear spin (^{13}C or ^{15}N). The black vertical arrows represent the spins state of the heteronuclear spin. The proton originally precesses in a clockwise direction. Inversion of the heteronuclear spin reverses the direction. If the inter-pulse delay is small compared to the J-coupling, the proton simply oscillates around the y-axis without undergoing any evolution due to J-coupling. Consequently its position in the spectrum is defined solely by its chemical shift and no splitting of the line occurs.

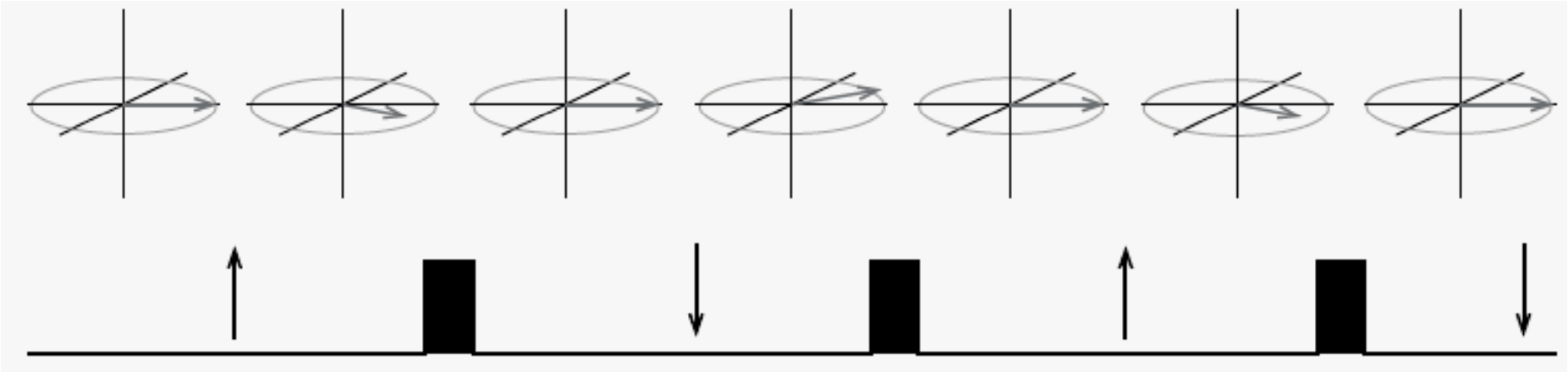

7.4.2 Decoupling Methods

Due to resonance off-set effects, the simple inversion of the coupled partner by the application of 180° pulses is very ineffective if the resonance frequency of the decoupled spin differs from the carrier frequency. Because of the wide frequency range of ^{13}C and ^{15}N spins it has been necessary to design more elaborate pulse sequences for decoupling of these nuclei.

The three commonly used decoupling schemes for isolated H-C and H-N spins are MLEV-16, WALTZ-16, and GARP-1. These schemes are usually provided with the software that accompanies the spectrometer or are easily programmed with the pulse program software. A detailed description of the development and properties of these schemes can be found in Freeman [56]. MLEV-16 is an early decoupling scheme whose properties are inferior to WALTZ and GARP and is only included here for purposes of comparison.

The schemes that have been designed for the decoupling of scalar coupled spins consist of a collection of three related schemes: DIPSI-1, DIPSI-2, and DIPSI-3 (Decoupling In the Presense of Scalar Interations) (Table 7.3). The three DIPSI sequences differ in the length of the fundamental rotation operator (see below) to accommodate timing limitations that Scalar Coupling 147 may occur in pulse sequences. DIPSI-1 is the shortest sequence and comparable to WALTZ-16 in overall length.

Each of these decoupling schemes are composed of a fundamental rotation operator, R, which is applied with various phases during decoupling. Each rotation operator, R, can be considered to be equivalent to a 180° pulse, causing inversion of the decoupled spin. In these decoupling schemes the rotation operators have been designed to be insensitive to resonance offset effects. The MLEV rotation operator is one of the simplest; a composite 180° pulse (Sec 6.3.3) or

$$[\frac{\pi}{2}]_x - [\pi]_y - [\frac{\pi}{2}]_x$$

The different rotational operators associated with each decoupling scheme is shown in Table 7.3. Additional insensitivity to resonance offset effects is obtained by forming a four element cycle of the basic rotation operator: $RR\bar{R}\bar{R}$
Where $\bar{R}$ is the inversion of R. In the case of MLEV and WALTZ decoupling, cyclic permutations of this basic cycle are combined to give a 16 step super-cycle,

$$RR\bar{R}\bar{R}\ \bar{R}RR\bar{R}\ \bar{R}\bar{R}RR\ R\bar{R}\bar{R}R$$

which further compensates for resonance-offset effects. The number of *R* elements in the super-cycle are often indicated in name of the decoupling scheme, e.g.
MLEV-4 $=RR\bar{R}\bar{R}$ and MLEV-16$=RR\bar{R}\bar{R}\ \bar{R}RR\bar{R}\ \bar{R}\bar{R}RR\ R\bar{R}\bar{R}R$.

Decoupling Scheme	*R Element*	Ξ	*Residual Line Broadening*	*Ref.*
MLEV-16	$[\pi/2]_x[\pi]_y[\pi/2]_x$	1.5	Large	[94]
WALTZ-16	$[\pi/2]_x[\pi]_{-x}[3\pi/2]_x$	1.8	Small	[147]
DISPI-1	$365\ \overline{295}\ 65\ \overline{305}\ 350$	0.8	Small	[148]
DISPI-2	$320\ \overline{410}\ 290\ \overline{285}\ 30\ \overline{245}\ 375\ \overline{265}\ 370$	1.2	Small	[148]
DISPI-3	$\overline{245}\ 395\ \overline{250}\ 275\ \overline{30}\ 230\ \overline{360}\ 245\ \overline{370}\ 340$ $\overline{350}\ 260\ \overline{270}\ 30\ \overline{225}\ 365\ \overline{255}\ 395$	1.6	Very Small	[148]
GARP-1	$R = \bar{P}Q\overline{PQ}$, overall cycle is $RR\bar{R}\bar{R}$ $P = 27.1\ \overline{57.6}\ 122.0$ $Q = \overline{120.8}\ 262.8\ \overline{65.9}\ 64.6$ $\overline{87.0}\ 90.0\ \overline{137.2}\ 256.2\ \overline{71.6}\ 51.1$	4.8	Moderate	[146]

Table 7.3. Decoupling schemes. The R element is the basic rotation operator that is used to form the $RR\overline{RR}$ decoupling element. Pulse angles and phases are indicated. In the case of DIPSI and GARP decoupling, the pulses are along the x-axis or along the minus x-axis if the angle is overlined. Angles are given in degrees. The figure of merit, Ξ, for each sequence is also provided. Finally, the quality of the decoupling is indicated by the residual line broadening; higher quality sequences have a smaller residual line broadening.

7.4.3 Performance of Decoupling Schemes

The frequency range over which the decoupling is effective is characterized by the bandwidth. Empirically, decoupling is considered to be effective if the intensity of the collapsed multiplet has at least 80% of the intensity of the fully decoupled signal. The bandwidth can be increased by using shorter pulses in the decoupling sequence. However, the additional power will cause sample heating, and in extreme cases can lead to equipment failure. Since the decoupling bandwidth is proportional to the field strength of the decoupling pulses, it is convenient to define a figure of merit, Ξ, as: $\Xi = \frac{2\pi\Delta F}{\gamma B}$

Where ΔF is the region over which the decoupling is effective (in Hz), and γB is the strength of the decoupling field (in units of rad/sec). Schemes that have a higher figure of merit can decouple a larger bandwidth for the same amount of RF power.

The Ξ values for MLEV-16, WALTZ-16, DIPSI-n, and GARP-1 decoupling are shown in Table 7.3. MLEV-16 has the smallest bandwidth while WALTZ-16 has a slightly larger bandwidth, but the quality of the decoupling is much higher (see below). GARP-1 has the largest bandwidth of the three schemes, but is of lower quality than WALTZ-16. The bandwidths of the DIPSI-n sequences depend on the length of the sequence with DIPSI-3 providing the largest bandwidth of the three. However, its bandwidth is still smaller than that of WALTZ-16.

In addition to differing in bandwidth, decoupling schemes also differ in the amount of residual coupling that remains in effect in the presence of the decoupling. The residual coupling will increase the apparent linewidth of the unresolved multiplet, causing a decrease the intensity of the observed peak. The amount of residual coupling depends on the decoupling scheme. WALTZ-16 has a much smaller residual bandwidth than GARP or MLEV-16, and therefore gives high quality decoupling. Of the DIPSI decoupling schemes, DIPSI-3 produces excellent decoupling in the case of scalar coupled systems, out-performing WALTZ-16.

7.4.3 Performance of Decoupling Schemes

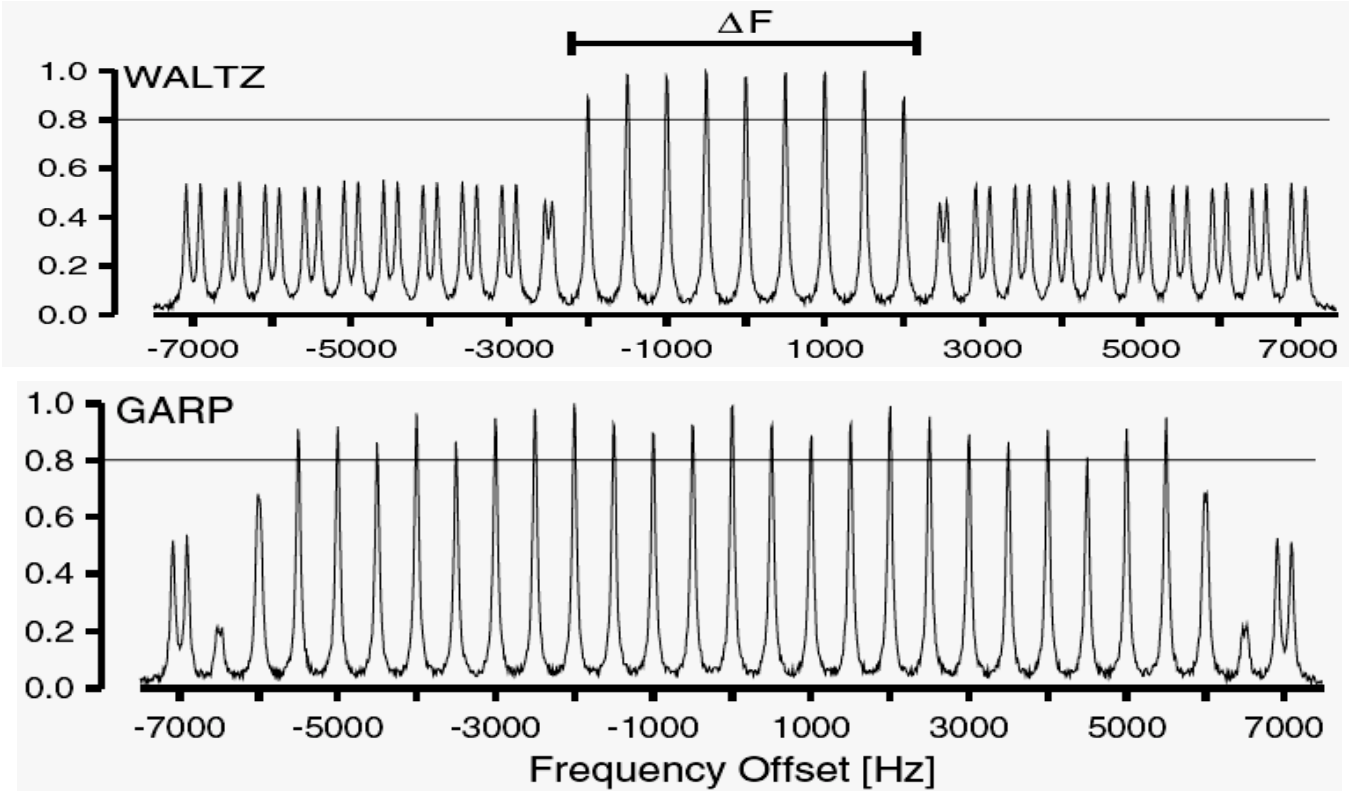

Figure 7.10. Bandwidth of WALTZ and GARP decoupling. A series of NMR spectra of a single amide proton, attached to an ^{15}N spin, are shown for different decoupler frequencies. The decoupler frequency is given relative to the frequency of the ^{15}N resonance. This frequency was varied in 500 Hz steps, ranging from 7000 Hz below (left) to 7000 Hz above the nitrogen frequency (right). In this illustration the bandwidth of the WALTZ decoupling is 4 kHz, while that for GARP decoupling is 11 kHz. In the case of GARP decoupling, the height of the proton lines are not uniform within the bandwidth due to a variation in the residual decoupling that depends on the frequency offset. In contrast, the height of the lines for WALTZ decoupling are uniform, indicating a small dependence of the residual coupling on the frequency offset.

Table 7.4. Guide to decoupling schemes.

Situation	*Decoupling Scheme*	*Rational*
Decouple ^{15}N, observe protons.	WALTZ-16.	Narrow bandwidth of ^{15}N, typically 30 ppm (ΔF = 1.8 kHz) with no ^{15}N-^{15}N coupling, WALTZ-16 provides excellent line-narrowing.
Decouple ^{13}C, observe protons.	GARP-1 for natural abundance.	Require high bandwidth to cover carbon spectrum. Typical bandwidth is 80 ppm ($\Delta F = 12$ kHz).
	DIPSI-3 for uniformly labeled samples, provided sufficient bandwidth can be generated. This will depend on the hardware and the desired bandwidth.	^{13}C-^{13}C couplings can interfere with GARP-1 decoupling.
Decouple ^{1}H, observe carbon or nitrogen.	DISPI-2 or DIPSI-3. Timing constraints may force the use of DIPSI-2 in triple resonance experiments.	Moderate proton bandwidth needed, 4 ppm ($\Delta F = 2.4$ kHz) for amides, 6 ppm for aliphatics ($\Delta F = 3.6$ kHz). ^{1}H-^{1}H couplings will interfere with WALTZ-16 and GARP-1.

Chapter 8 COUPLED SPINS: DENSITY MATRIX AND PRODUCT OPERATOR FORMALISM

In the previous chapter the coupling between two spins was analyzed using the wavefunctions associated with each of the quantum states. This type of analysis is quite satisfactory for determining the appearance of the one-dimensional NMR spectrum of the coupled spins. However, this approach is completely impractical for calculations on an ensemble of spins that are subject to multiple excitation pulses in typical NMR experiments. Consequently, we return to the density matrix to analyze the evolution of the coupled spins. In this analysis we will only assume weak coupling, of the AX kind. This assumption is not a severe restriction since heteronuclear couplings, such as between protons and carbon or carbon and nitrogen, are those that are used for magnetization transfer by various NMR experiments.

8.1 Density Matrix for Two Coupled Spins

For two coupled spins the wavefunctions are a linear combination of the four basis vectors: $\Psi = c_1|\alpha\alpha\rangle + c_2|\alpha\beta\rangle + c_3|\beta\alpha\rangle + c_4|\beta\beta\rangle$
and the density matrix is now a 4x4 matrix:

$$\rho = \begin{bmatrix} c_1c_1^* & c_1c_2^* & c_1c_3^* & c_1c_4^* \\ c_2c_1^* & c_2c_2^* & c_2c_3^* & c_2c_4^* \\ c_3c_1^* & c_3c_2^* & c_3c_3^* & c_3c_4^* \\ c_4c_1^* & c_4c_2^* & c_4c_3^* & c_4c_4^* \end{bmatrix}$$

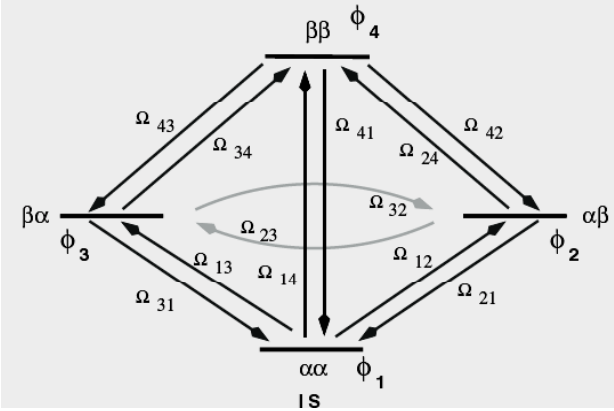

	αα	αβ	βα	ββ
αα	P_1	Ω_{12}	Ω_{13}	Ω_{14}
αβ	Ω_{21}	P_2	Ω_{23}	Ω_{24}
βα	Ω_{31}	Ω_{32}	P_3	Ω_{34}
ββ	Ω_{41}	Ω_{42}	Ω_{43}	P_4

Each of the 16 elements in this density matrix provides information on various states of the system. The nature of the information contained in each element can be identified from its time evolution under the Hamiltonian.

This time dependence is given by: $$i\hbar\frac{d\rho_{nm}}{dt} = (E_n - E_m)\rho_{nm}$$

Or in frequency unit: $$\frac{d\rho_{nm}}{dt} = -i(\Omega_n - \Omega_m)\rho_{nm}$$

For two coupled spins, the individual elements of the density matrix will evolve with the frequencies given in Table 8.1. For example, given an initial value of $c_1c^*_3(t = 0)$, the values of this element of the density matrix at some future time is:

$$c_1c^*_3(t) = e^{i(\omega I - \pi J)t}c_1c^*_3(t = 0)$$

	$\alpha\alpha$	$\alpha\beta$	$\beta\alpha$	$\beta\beta$
$\alpha\alpha$	0	$\omega_S - \pi J$	$\omega_I - \pi J$	$\omega_I + \omega_S$
$\alpha\beta$	$-\omega_S + \pi J$	0	$\omega_I - \omega_S$	$\omega_I + \pi J$
$\beta\alpha$	$-\omega_I + \pi J$	$-\omega_I + \omega_S$	0	$\omega_S + \pi J$
$\beta\beta$	$-\omega_I - \omega_S$	$-\omega_I - \pi J$	$-\omega_S - \pi J$	0

Table 8.1. Time evolution of the elements of the density matrix. The frequency at which an element of the density matrix evolves is indicated. The row indicates the ground state and the column indicates the excited state. For example, the element of the density matrix that represents the double quantum transition from the αα ground state to the ββ double quantum state will evolve at a frequency of $\omega = \omega_I + \omega_S$.

The 16 elements of the density matrix can be divided into four distinct groups. The four diagonal elements, $c_i c^*_i$, do not evolve with time and therefore refer to the population of the ψ_i state. The off-diagonal elements indicate the presence of coherently excited states or transitions. These transitions can be divided into zero quantum, single quantum, and double quantum transitions:

- **Zero quantum transitions**, **or coherences**, are those whose frequency is given by the difference in the resonance frequency between the I and S spins (Flip-flop). These transitions connect the αβ and βα states. Zero quantum transitions correspond to spin-spin flips, or an interchange of m_z values. There is no net change in the overall quantum number. The zero-quantum transitions are indicated as Ω_{23} and Ω_{32} in Fig. 8.1.
- **Single quantum transitions**, or coherences, change m_z for one of the two spins (Flip). These transitions form the outer set of arrows in Fig. 8.1.
- **Double quantum transitions,** or coherences, involve a change in m_z for both spins (Flop-flop). The two double quantum transitions connect the ββ state to the αα state.

8.2 Product Operator Representation of the Density Matrix

In the case of a single spin it was possible to describe the density matrix in terms of a group of four product operators: E, I_x, I_y and I_z.

For two uncoupled spins, I and S, we can also write two sets of product operators that can be used to represent the density matrices associated with the two spins:

E, I_x, I_y, I_z, S_x, S_y and S_z.

However, these set of seven density matrices will not be sufficient to describe a coupled system because the Hamiltonian for the scalar coupling is the product of two operators:

$$\mathcal{H} = 2\pi J I_z S_z$$

A closed group of product operators that can be used to describe any arbitrary density matrix for two coupled spins is generated by taking all possible products of the single spin operators. This forms a set of 16 product operators:

$1/2E$	I_x	I_y	I_z
S_x	$2I_xS_x$	$2I_yS_x$	$2I_zS_x$
S_y	$2I_xS_y$	$2I_yS_y$	$2I_zS_y$
S_z	$2I_xS_z$	$2I_yS_z$	$2I_zS_z$

The matrix form of these density matrices is found by forming the tensor or direct product between pairs of single-spin 2x2 matrices. This is equivalent to taking all possible combinations of the elements in each 2x2 matrix. The direct product of two single spin operators is calculated as follows.

Consider two operators, OA and OB: $\mathcal{O}_A = \begin{bmatrix} a & b \\ c & d \end{bmatrix}, \mathcal{O}_B = \begin{bmatrix} e & f \\ g & h \end{bmatrix}$

Then the direct product of the two operators, $\mathcal{O}_A \otimes \mathcal{O}_B$, is obtained as follows:

$$\mathcal{O}_{AB} = \mathcal{O}_A \otimes \mathcal{O}_B = \begin{bmatrix} a & b \\ c & d \end{bmatrix} \otimes \begin{bmatrix} e & f \\ g & h \end{bmatrix} = \begin{bmatrix} a\begin{bmatrix} e & f \\ g & h \end{bmatrix} & b\begin{bmatrix} e & f \\ g & h \end{bmatrix} \\ c\begin{bmatrix} e & f \\ g & h \end{bmatrix} & d\begin{bmatrix} e & f \\ g & h \end{bmatrix} \end{bmatrix} = \begin{bmatrix} ae & af & be & bf \\ ag & ah & bg & bh \\ ce & cf & de & df \\ cg & ch & dg & dh \end{bmatrix}$$

Any pair of operators can be combined to give the resultant direct product. For example:

$$I_xS_y = I_x \otimes S_y = \frac{1}{2}\begin{bmatrix} 0 & 1 \\ 1 & 0 \end{bmatrix} \otimes \frac{1}{2}\begin{bmatrix} 0 & -i \\ i & 0 \end{bmatrix} = \frac{1}{4}\begin{bmatrix} 0 & 0 & 0 & -i \\ 0 & 0 & i & 0 \\ 0 & -i & 0 & 0 \\ i & 0 & 0 & 0 \end{bmatrix}$$

Single spin operators can also be written in the same representation as the two coupled spins by taking the direct product with the identity matrix:

$$I_z = I_z \otimes 1 = \frac{1}{2}\begin{bmatrix} 1 & 0 \\ 0 & -1 \end{bmatrix} \otimes \begin{bmatrix} 1 & 0 \\ 0 & 1 \end{bmatrix} = \begin{bmatrix} 1 & 0 & 0 & 0 \\ 0 & 1 & 0 & 0 \\ 0 & 0 & -1 & 0 \\ 0 & 0 & 0 & -1 \end{bmatrix}$$

Table 8.2. The complete set of 16 product operators

$$\frac{1}{2}E = \frac{1}{2}\begin{bmatrix} 1 & 0 & 0 & 0 \\ 0 & 1 & 0 & 0 \\ 0 & 0 & 1 & 0 \\ 0 & 0 & 0 & 1 \end{bmatrix} \qquad 2I_zS_z = \frac{1}{2}\begin{bmatrix} 1 & 0 & 0 & 0 \\ 0 & -1 & 0 & 0 \\ 0 & 0 & -1 & 0 \\ 0 & 0 & 0 & 1 \end{bmatrix} \qquad 2I_xS_x = \frac{1}{2}\begin{bmatrix} 0 & 0 & 0 & 1 \\ 0 & 0 & 1 & 0 \\ 0 & 1 & 0 & 0 \\ 1 & 0 & 0 & 0 \end{bmatrix} \qquad 2I_yS_y = \frac{1}{2}\begin{bmatrix} 0 & 0 & 0 & -1 \\ 0 & 0 & 1 & 0 \\ 0 & 1 & 0 & 0 \\ -1 & 0 & 0 & 0 \end{bmatrix}$$

$$I_x = \frac{1}{2}\begin{bmatrix} 0 & 0 & 1 & 0 \\ 0 & 0 & 0 & 1 \\ 1 & 0 & 0 & 0 \\ 0 & 1 & 0 & 0 \end{bmatrix} \qquad S_x = \frac{1}{2}\begin{bmatrix} 0 & 1 & 0 & 0 \\ 1 & 0 & 0 & 0 \\ 0 & 0 & 0 & 1 \\ 0 & 0 & 1 & 0 \end{bmatrix} \qquad 2I_xS_z = \frac{1}{2}\begin{bmatrix} 0 & 0 & 1 & 0 \\ 0 & 0 & 0 & -1 \\ 1 & 0 & 0 & 0 \\ 0 & -1 & 0 & 0 \end{bmatrix} \qquad 2I_yS_z = \frac{1}{2}\begin{bmatrix} 0 & 0 & -i & 0 \\ 0 & 0 & 0 & i \\ i & 0 & 0 & 0 \\ 0 & -i & 0 & 0 \end{bmatrix}$$

$$I_y = \frac{1}{2}\begin{bmatrix} 0 & 0 & -i & 0 \\ 0 & 0 & 0 & -i \\ i & 0 & 0 & 0 \\ 0 & i & 0 & 0 \end{bmatrix} \qquad S_y = \frac{1}{2}\begin{bmatrix} 0 & -i & 0 & 0 \\ i & 0 & 0 & 0 \\ 0 & 0 & 0 & -i \\ 0 & 0 & i & 0 \end{bmatrix} \qquad 2I_zS_x = \frac{1}{2}\begin{bmatrix} 0 & 1 & 0 & 0 \\ 1 & 0 & 0 & 0 \\ 0 & 0 & 0 & -1 \\ 0 & 0 & -1 & 0 \end{bmatrix} \qquad 2I_xS_y = \frac{1}{2}\begin{bmatrix} 0 & 0 & 0 & -i \\ 0 & 0 & i & 0 \\ 0 & -i & 0 & 0 \\ i & 0 & 0 & 0 \end{bmatrix}$$

$$I_z = \frac{1}{2}\begin{bmatrix} 1 & 0 & 0 & 0 \\ 0 & 1 & 0 & 0 \\ 0 & 0 & -1 & 0 \\ 0 & 0 & 0 & -1 \end{bmatrix} \qquad S_z = \frac{1}{2}\begin{bmatrix} 1 & 0 & 0 & 0 \\ 0 & -1 & 0 & 0 \\ 0 & 0 & 1 & 0 \\ 0 & 0 & 0 & -1 \end{bmatrix} \qquad 2I_zS_y = \frac{1}{2}\begin{bmatrix} 0 & -i & 0 & 0 \\ i & 0 & 0 & 0 \\ 0 & 0 & 0 & i \\ 0 & 0 & -i & 0 \end{bmatrix} \qquad 2I_yS_x = \frac{1}{2}\begin{bmatrix} 0 & 0 & 0 & -i \\ 0 & 0 & -i & 0 \\ 0 & i & 0 & 0 \\ i & 0 & 0 & 0 \end{bmatrix}$$

8.2.1 Detectable Elements of ρ

The density matrix contains information on populations, zero-quantum, single-quantum, and double-quantum transitions. Only a sub-set of these can be detected by the instrument. Quadrature detection measures $M_x + iM_y$, or equivalently, $[I_x + S_x] + i[I_y + S_y]$, which is equal to $I^+ + S^+$. Consequently, the detected signal is given by: Trace(ρ $[I^+ + S^+]$).

The above trace is only non-zero for the density matrices I_x, I_y, S_x, and S_y. In addition, the density matrices represented by the lowering operators, I^- and S^- can also be detected. All other density matrices will give no detectable signal.

However, we shall see later that density matrices that contain one transverse operator and one longitudinal operator, for example, $2I_xS_z$ can evolve into a detectable signal due to J-coupling.

Whether a particular product operator representation of the density matrix can be detected is determined by simply calculating Trace(ρ [I^+ +S^+]). The matrix form of I^+ and S^+ are obtained by adding $I_x + iI_y$ and $S_x + iS_y$, giving:

$$I^+ = \begin{bmatrix} 0 & 0 & 1 & 0 \\ 0 & 0 & 0 & 1 \\ 0 & 0 & 0 & 0 \\ 0 & 0 & 0 & 0 \end{bmatrix} \qquad S^+ = \begin{bmatrix} 0 & 1 & 0 & 0 \\ 0 & 0 & 0 & 0 \\ 0 & 0 & 0 & 1 \\ 0 & 0 & 0 & 0 \end{bmatrix}$$

As examples, we first show that the density matrices, represented by I_x or I^-, give a detectable signal.

$$\text{Signal}(I_x) = \text{Trace}(\rho\,[I^+ + S^+]) = \text{Trace}(I_x\,[I^+ + S^+])$$

$$= \text{Trace}\left(\begin{bmatrix} 0 & 0 & 1 & 0 \\ 0 & 0 & 0 & 1 \\ 1 & 0 & 0 & 0 \\ 0 & 1 & 0 & 0 \end{bmatrix}\begin{bmatrix} 0 & 1 & 1 & 0 \\ 0 & 0 & 0 & 1 \\ 0 & 0 & 0 & 1 \\ 0 & 0 & 0 & 0 \end{bmatrix}\right) = \text{Trace}\left(\begin{bmatrix} 0 & 0 & 0 & 1 \\ 0 & 0 & 0 & 0 \\ 0 & 1 & 1 & 0 \\ 0 & 0 & 0 & 1 \end{bmatrix}\right) = 0 + 0 + 1 + 1 = 2$$

Signal(I^-) = Trace(ρ [I^+ + S^+]) = Trace(I− [I^+ + S^+])

$$= \text{Trace}\left(\begin{bmatrix} 0 & 0 & 0 & 0 \\ 0 & 0 & 0 & 0 \\ 1 & 0 & 0 & 0 \\ 0 & 1 & 0 & 0 \end{bmatrix}\begin{bmatrix} 0 & 1 & 1 & 0 \\ 0 & 0 & 0 & 1 \\ 0 & 0 & 0 & 1 \\ 0 & 0 & 0 & 0 \end{bmatrix}\right) = \text{Trace}\left(\begin{bmatrix} 0 & 0 & 0 & 0 \\ 0 & 0 & 0 & 0 \\ 0 & 0 & 1 & 0 \\ 0 & 0 & 0 & 1 \end{bmatrix}\right) = 0 + 0 + 1 + 1 = 2$$

In contrast, the density matrices represented by I^+, $2I_xS_z$, or $2I_xS_y$, do not give a detectable signal: (Not shown)

In summary, the relationships between the density matrix and the detected signals are:

1. Density matrices that are represented by product operators consisting of one transverse operator, e.g. Ix, represent single quantum transitions and yield a detectable signal. In the case of quadrature detection, I– and S–, are the detected signals.
2. Density matrices that are represented by product operators consisting of one transverse operator and one z-operator, e.g. 2IxSz, are not directly detectable, but can evolve into detectable magnetization due to J-coupling. Product operators of this type represent undetectable single-quantum transitions.
3. Density matrices that are represented by product operators consisting entirely of z-operators, e.g. Iz, Sz, IzSz represent populations or zero quantum transitions and therefore cannot be detected.
4. Density matrices that represent product operators consisting of two transverse terms, e.g. 2IxSy, represent double quantum transitions that do not give rise to detectable transitions.

8.3 Density Matrix Treatment of two coupled spins in a One-pulse Experiment

Example: Two coupled protons. I and S. Both spins are excited by a 90◦ pulse along the x-axis and the resulting signal is detected after excitation. The evolution of the density matrix during this experiment can be represented as follows: $\rho_o \xrightarrow{P_X} \rho_1 \xrightarrow{\mathcal{H}} \rho_1(t)$

The excitation is a rotation of the density matrix: $\rho_1 = R_x(\pi/2)\rho_o R_x^\dagger(\pi/2)$

During detection, the density matrix will evolve under the complete Hamiltonian, $H = -\omega_I I_z - \omega_S S_z + 2\pi J I_z S_z$, as follows: $\rho_1(t) = e^{-i\mathcal{H}t}\rho_1 e^{+i\mathcal{H}t}$

With the final detected signals given by: $S(t) = \mathrm{Trace}(\rho_1(t)\ [I^+ + S^+])$

$$\rho_o \;=\; I_z + S_z \;=\; I_z \otimes 1 + 1 \otimes S_z = \frac{1}{2}\begin{bmatrix} 1 & 0 & 0 & 0 \\ 0 & 1 & 0 & 0 \\ 0 & 0 & -1 & 0 \\ 0 & 0 & 0 & 1 \end{bmatrix} + \frac{1}{2}\begin{bmatrix} 1 & 0 & 0 & 0 \\ 0 & -1 & 0 & 0 \\ 0 & 0 & 1 & 0 \\ 0 & 0 & 0 & -1 \end{bmatrix} = \begin{bmatrix} 1 & 0 & 0 & 0 \\ 0 & 0 & 0 & 0 \\ 0 & 0 & 0 & 0 \\ 0 & 0 & 0 & -1 \end{bmatrix}$$

The rotation matrix, Rx(π/2) is obtained from the single-spin rotation matrix for an x-rotation in a similar fashion (Both I and S spins are affected by the 90° pulse):

$$R_x^{IS}(\pi/2) \;=\; R_x^I(\pi/2) \otimes R_x^S(\pi/2)$$

$$= \frac{1}{\sqrt{2}}\begin{bmatrix} 1 & -i \\ -i & 1 \end{bmatrix} \otimes \frac{1}{\sqrt{2}}\begin{bmatrix} 1 & -i \\ -i & 1 \end{bmatrix} = \frac{1}{2}\begin{bmatrix} 1 & -i & -i & -1 \\ -i & 1 & -1 & -i \\ -i & -1 & 1 & -i \\ -1 & -i & -i & 1 \end{bmatrix}$$

Calculation of ρ_1:

$$\rho_1 \;=\; R_x(\pi/2)\rho_o R_x^\dagger(\pi/2) = \left(\frac{1}{2}\right)^2 \begin{bmatrix} 1 & -i & -i & -1 \\ -i & 1 & -1 & -i \\ -i & -1 & 1 & -i \\ -1 & -i & -i & 1 \end{bmatrix} \begin{bmatrix} 1 & 0 & 0 & 0 \\ 0 & 0 & 0 & 0 \\ 0 & 0 & 0 & 0 \\ 0 & 0 & 0 & -1 \end{bmatrix} \begin{bmatrix} 1 & i & i & -1 \\ i & 1 & -1 & i \\ i & -1 & 1 & i \\ -1 & i & i & 1 \end{bmatrix}$$

$$= \left(\frac{1}{2}\right)^2 \begin{bmatrix} 0 & 2i & 2i & 0 \\ -2i & 0 & 0 & 2i \\ -2i & 0 & 0 & 2i \\ 0 & -2i & -2i & 0 \end{bmatrix} = \frac{1}{2}\begin{bmatrix} 0 & i & i & 0 \\ -i & 0 & 0 & i \\ -i & 0 & 0 & i \\ 0 & -i & -i & 0 \end{bmatrix} \;=\; -I_y - S_y$$

Evolution of the Density Matrix during Detection: $\rho_1(t) = e^{-i\mathcal{H}t}\rho_1 e^{+i\mathcal{H}t}$

$$\rho_1(t) = \begin{bmatrix} 0 & ie^{i(+\omega_S - \pi J)t} & ie^{i(+\omega_I - \pi J)t} & 0 \\ -ie^{i(-\omega_S + \pi J)t} & 0 & 0 & ie^{i(+\omega_I + \pi J)t} \\ -ie^{i(-\omega_I + \pi J)t} & 0 & 0 & ie^{i(+\omega_S + \pi J)t} \\ 0 & -ie^{i(-\omega_I - \pi J)t} & -ie^{i(-\omega_S - \pi J)t} & 0 \end{bmatrix}$$

The final detected signal is given by Trace(ρ [I+ + S+]). To simplify the calculation, the signal associated with only the I spin will be calculated. We first calculate ρI^+:

$$\rho I^+ = \begin{bmatrix} 0 & ie^{i(+\omega_S-\pi J)t} & ie^{i(+\omega_I-\pi J)t} & 0 \\ -ie^{i(-\omega_S+\pi J)t} & 0 & 0 & ie^{i(+\omega_I+\pi J)t} \\ -ie^{i(-\omega_I+\pi J)t} & 0 & 0 & ie^{i(+\omega_S+\pi J)t} \\ 0 & -ie^{i(-\omega_I-\pi J)t} & -ie^{i(-\omega_S-\pi J)t} & 0 \end{bmatrix} \begin{bmatrix} 0 & 0 & 1 & 0 \\ 0 & 0 & 0 & 1 \\ 0 & 0 & 0 & 0 \\ 0 & 0 & 0 & 0 \end{bmatrix}$$

$$= \begin{bmatrix} 0 & 0 & 0 & ie^{i(+\omega_S-\pi J)t} \\ 0 & 0 & -ie^{i(-\omega_S+\pi J)t} & 0 \\ 0 & 0 & -ie^{i(-\omega_I+\pi J)t} & 0 \\ 0 & 0 & 0 & -ie^{i(-\omega_I-\pi J)t} \end{bmatrix}$$

The trace gives the detected signal (ignoring the sign of ω):

$$\mathrm{Trace}(\rho\, I^+) = -i[e^{i(\omega_I+\pi J)t} + e^{i(\omega_I-\pi J)t}]$$

The amplitude "i" simply represents a phase shift of the signal and can be ignored. The remaining part of the expression represents two spectral lines, centered around ω_I and separated by a total of 2πJ rad/sec. Repeating this calculation using S^+ would yield a similar result, with ω_I replaced by ω_S. The final detected signal contains four resonance lines, doublets at ω_I and ω_S, with each doublet split by J Hz:

$$S(t) = e^{i(\omega_I+\pi J)t} + e^{i(\omega_I-\pi J)t} + e^{i(\omega_S+\pi J)t} + e^{i(\omega_S-\pi J)t}$$

8.4 Manipulation of Two-spin Product Operators

The above manipulations of the 4x4 density matrix are even more tedious than the manipulation of the simpler 2x2 density matrix for uncoupled spins. The representation of the density matrix by a linear combination of product operators greatly simplifies the calculation of ρ at various positions in the NMR experiment.

Since there are now two coupled spins, we also have to determine how to apply these rules to products of operators. In addition, it is also necessary to consider the effect of the J-coupling term in the Hamiltonian, $2\pi J I_z S_z$, on the evolution of the density matrix under free precession. Rules for determining how the density matrix is modified by pulses and free precession are as follows:

1. If operators P and Q commute (i.e. belong to different spins) , then a rotation operator associated with one spin has no effect on the density matrix that corresponds to the other spin. For example, a proton pulse has no effect on the density matrix that represents magnetization associated with carbon or nitrogen spins.

$$e^{-i\theta P} Q e^{i\theta P} \quad = \quad Q e^{-i\theta P} e^{i\theta P} \quad = \quad Q$$

2. The one spin component of an evolving product operator can be treated separately:

$$2I_y S_z \overset{\beta(I_x+S_x)}{\longrightarrow} 2\left[I_y cos(\beta) + I_z sin(\beta)\right]\left[S_z cos(\beta) - S_y sin(\beta)\right]$$

For example, a 90°x pulse, applied to both spins, gives: $2I_yS_z \rightarrow -2I_zS_y$

3. One-spin operators (e.g. I_x), that are found as part of the rotation angle are taken as constants in the expression. The usual application of this rule is to evaluate the effect of J-coupling on evolution of the density matrix. For example, the effect of J-coupling on the evolution of protons (I spins) is equivalent to a rotation about the z-axis by an angle $2\pi J S_z t$, $e^{-i2\pi J I_z S_z} = e^{-i(2\pi J S_z t) I_z}$

The difficulty with this expression is that there is now an operator, S_z, that is part of an argument for a trigonometric function. The operators are taken out of the argument using the series expansion for each term:

$$cos(\pi Jt2S_z) = 1 - \frac{(\pi J2t)^2}{2!}S_z^2 + \frac{(\pi J2t)^4}{4!}S_z^4 \ldots = 1 - \frac{(\pi J2t)^2}{2!}\left[\frac{1}{4}\right] + \frac{(\pi J2t)^4}{4!}\left[\frac{1}{4}\right]^2 \ldots$$

$$= cos(\pi Jt)$$

Similarly:

$$sin(\pi Jt2S_z) = \frac{\pi J2t}{1}S_z - \frac{(\pi J2t)^3}{3!}S_z^3 + \frac{(\pi J2t)^5}{5!}S_z^5 = 2S_z sin(\pi Jt)$$

Thus:

$$I_x \xrightarrow{2\pi JtI_zS_z} I_x cos(\pi Jt) + 2I_y S_z sin(\pi Jt)$$

4. The evolution of a product of two operators under J-coupling would be evaluated using a combination of rule 2 and rule 3. First consider the evolution of 2IySz:

$2I_yS_z \xrightarrow{J} 2[I_y cos(\pi JtS_z) - I_x sin(\pi JtS_z)] \times S_z = 2[I_y cos(\pi Jt) - I_x S_z sin(\pi Jt)] \times S_z$

$= 2I_yS_z cos(\pi Jt) - 2I_x S^2{}_z \, sin(\pi Jt) = 2I_yS_z cos(\pi Jt) - I_x sin(\pi Jt)$

The product of two transverse operators is evaluated in exactly the same way:

$2I_xS_y \xrightarrow{J} 2\,[I_x cos(\pi Jt) + 2I_yS_z sin(\pi Jt)] \times [S_y cos(\pi Jt) - 2I_zS_x sin(\pi Jt)]$

It can be shown that product operators containing two transverse terms, such as $2I_xS_y$, do not evolve under J-coupling .

8.5. Transformations of Two-spin Product Operators:

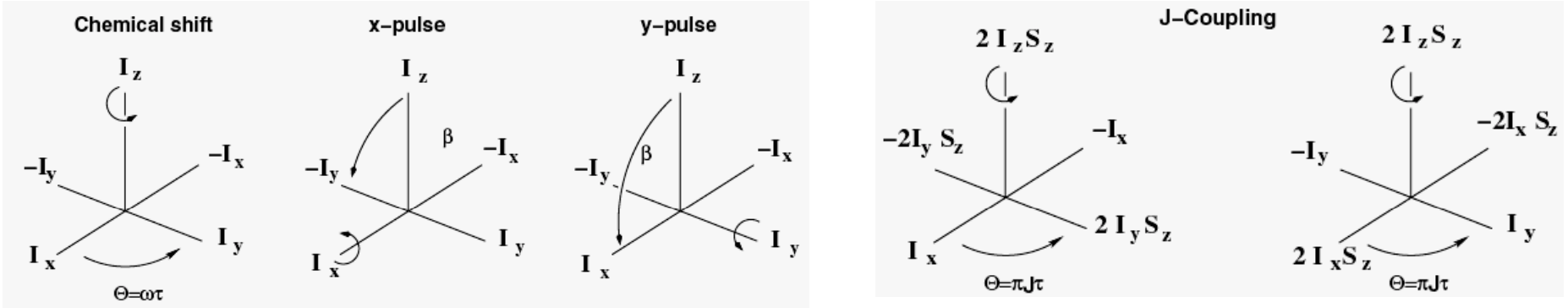

Figure 8.2 Manipulation of the density matrices using the product operator representation. The left figure shows the effect of chemical shift evolution (e.g. $H = \omega_I I_z$), with a rotation angle of ωt. The effects of pulses, with a flip angle of β degrees, are also shown on the middle left of the figure for pulses along the x-axis (middle), or y-axis (right). The effects of J-coupling on the density matrix are shown on the right of the figure, for the density matrix represented by I_x (left), or I_y (right). Here, the rotation angle is πJt.

Examples:

$$I_y \xrightarrow{\omega_I t} I_y cos(\omega_I t) - I_x sin(\omega_I t) \qquad I_y \xrightarrow{\beta_x} I_y cos(\beta) + I_z sin(\beta)$$

$$I_z \xrightarrow{\beta_y} I_z cos(\beta) + I_x sin(\beta) \qquad I_y \xrightarrow{2\pi J I_z S_z} I_y cos(\pi J t) - 2I_x S_z sin(\pi J t)$$

Note that in all cases the new density matrix, ρ, is a linear combination of the cosine weighted initial density matrix, ρi, plus the sine weighted density matrix that is advanced by 90°, ρ_{90}: $\rho_i \rightarrow \rho_i cos(\alpha t) + \rho_{90} sin(\alpha t)$

As time passes, the system will pass through all four forms of the density matrices that are in the same plane within Fig. 8.2.

$$I_x \rightarrow 2I_y S_z \rightarrow -I_x \rightarrow -2I_y S_z \rightarrow I_x \rightarrow 2I_y S_z ...$$

Transverse magnetization that is associated with a single spin operator, for example **I_x**, *is* often referred to as **in-phase magnetization**. In-phase magnetization evolves under the influence of Jcoupling to **anti-phase magnetization, 2IySz.** A vector model that represents this evolution is illustrated in Fig. 8.3. This representation shows why anti-phase magnetization cannot be detected. the individual vector components of the anti-phase magnetization cancel each other.

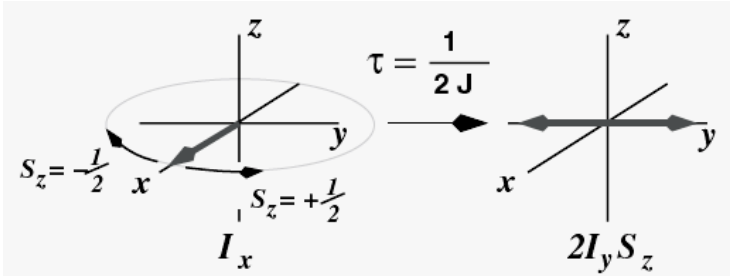

Figure 8.3. Inter-conversion of in-phase and antiphase magnetization. In-phase magnetization, I_x, evolves under J-coupling to produce anti-phase magnetization, $2I_yS_z$. In this representation the vector components of the anti-phase magnetization evolve in opposite directions because of the opposite spin states of S_z (m_z = +1/2 or m_z = −1/2).

8.6 Product Operator Treatment of a One-pulse Experiment

The product operator treatment of the one-pulse experiment for two coupled spins is similar to that utilized for a single isolated spin. As before, the NMR experiment transforms the initial density matrix, ρ_o, to $\rho_1(t)$ and the final detected signal is extracted from the final density matrix. The only complication is that it is necessary to keep track of two spins, I and S. Analysis of each step of the one-pulse experiment is discussed below.

Initial Product Operator: As discussed above, ρo = Iz + Sz.

Effect of 90◦ Pulse: We assume that this is a homonuclear experiment, **therefore the** pulse is applied to both spins. Assuming a perfect 90◦ pulse: $\rho_o \rightarrow \rho_1$

Or $\rho_o = I_z + S_z \xrightarrow{P_x(\pi/2)} -I_y - S_y = \rho_1$

Free Precession: The free precession of the spins causes the density matrix to evolve according to:

$$\rho_1(t) = e^{-iHt}\rho_1 e^{iHt} = e^{-i(\omega_I I_z+\omega_S S_z+2\pi J I_z S_z)t}\rho_1 e^{+i(\omega_I I_z+\omega_S S_z+2\pi J I_z S_z)t}$$

$$= e^{-i\omega_I I_z t}e^{-i\omega_S S_z t}e^{-i2\pi J I_z S_z t}\rho_1 e^{+i\omega_I I_z t}e^{+i\omega_S S_z t}e^{+i2\pi J I_z S_z t}$$

$$= e^{-i\omega_I I_z t}e^{-i\omega_S S_z t}\left[e^{-i2\pi J I_z S_z t}\rho_1 e^{+i2\pi J I_z S_z t}\right]e^{+i\omega_I I_z t}e^{+i\omega_S S_z t}$$

The middle term is jus the evolution due to J-coupling and can be written as:

$$-I_y - S_y \xrightarrow{J} [-I_y cos(\pi Jt) + 2I_x S_z sin(\pi Jt)] + [-S_y cos(\pi Jt) + 2S_x I_z(\pi Jt)]$$

The evolution of each other terms due to chemical shift is as follow:

$\rho_1(t) = -\cos(\pi Jt)\,[I_y\cos(\omega_I t) - I_x\sin(\omega_I t)] + 2S_z\sin(\pi Jt)\,[I_x\cos(\omega_I t) + I_y\sin(\omega_I t)]$
$- \cos(\pi Jt)\,[S_y\cos(\omega_S t) - S_x\sin(\omega_S t)] + 2I_z\sin(\pi Jt)\,[S_x\cos(\omega_I t) + S_y\sin(\omega_I t)]$

Collecting terms:

$\rho_1(t) = -I_y\cos(\omega_I t)\cos(\pi Jt) + I_x\sin(\omega_I t)\cos(\pi Jt) - S_y\cos(\omega_S t)\cos(\pi Jt)$
$+ S_x\sin(\omega_S t)\cos(\pi Jt) + 2I_x S_z\cos(\omega_I t)\sin(\pi Jt) + 2I_y S_z\sin(\omega_I t)\sin(\pi Jt)$
$+ 2S_x I_z\cos(\omega_S t)\sin(\pi Jt) + 2S_y I_z\sin(\omega_S t)\sin(\pi Jt)$

Since the only density matrices that give rise to detectable signal are represented by single transverse operators it is necessary to only focus on the first two lines of the above equation. Additional simplification is obtained if the transverse operators are written in the form of raising and lowering operators:

$$\rho_1(t) = \left[-\frac{1}{2i}(I^+ - I^-)cos(\omega_I t) + \frac{1}{2}(I^+ + I^-)sin(\omega_I t)\right]cos(\pi Jt)$$

$$+ \left[-\frac{1}{2i}(S^+ - S^-)cos(\omega_S t) + \frac{1}{2}(S^+ + S^-)sin(\omega_S t)\right]cos(\pi Jt)$$

Since the only components of the density matrix that gives rise to detectable signal are I^- and S−, it is only necessary to consider these two density matrices.

$$\rho_1(t) = I^- \left[\frac{cos(\omega_I t)}{2i} + \frac{sin(\omega_I t)}{2}\right] cos(\pi J t) \quad + S^- \left[\frac{cos(\omega_S t)}{2i} + \frac{sin(\omega_S t)}{2}\right] cos(\pi J t)$$

$$= I^- \frac{1}{2i} e^{i\omega_I t} cos(\pi J t) + S^- \frac{1}{2i} e^{i\omega_S t} cos(\pi J t)$$

Therefore, the detected signal is: $S(t) = \frac{1}{2i} e^{i\omega_I t} cos(\pi J t) + \frac{1}{2i} e^{i\omega_S t} cos(\pi J t)$

The Fourier transform of $e^{i\omega_I t}$ gives a single peak at ω_I and the $e^{i\omega_s t}$ term gives a single peak at ω_S. Each of these terms in the time domain is multiplied by cos(πJt), therefore the peaks at ω_I and ω_S will be convoluted with the Fourier transform of cos(πJt), resulting in the splitting of each peak by 2πJ. This gives the normal four line AX type spectrum, with a separation of 2πJ between each set of doublets.